J Sol-Gel Sci Techn (2006) 40:15–23
DOI 10.1007/s10971-006-8267-0

Synthesis of high surface area nanocrystalline anatase-TiO_2 powders derived from particulate sol-gel route by tailoring processing parameters

M. R. Mohammadi · M. C. Cordero-Cabrera · M. Ghorbani · D. J. Fray

Received: 25 October 2005 / Accepted: 13 March 2006 / Published online: 15 July 2006

Abstract Stabilised titania sols were prepared using an additive free particulate sol-gel route, via electrostatic stabilisation mechanism, with various processing parameters. Peptisation temperature, 50°C and 70°C, and TiO_2 concentration, 0.1, 0.2 and 0.4 molar, were chosen as processing parameters during sol preparation. Results from TiO_2 particle size and zeta potential of sols revealed that the smallest titania hydrodynamic diameter (13 nm) and the highest zeta potential (47.7 mV) were obtained for the sol produced at the lower peptisation temperature of 50°C and lower TiO_2 concentration of 0.1 M. On the other hand, between the sols prepared at 70°C, smaller titania particles (20 nm) and higher zeta potential (46.3 mV) were achieved with increasing TiO_2 concentration up to 0.4 M. X-ray diffraction (XRD) and Brunauer-Emmett-Teller (BET) results of produced powders annealed at different temperatures showed that the 300°C annealed powder made from 0.1 M sol prepared at 50°C was a mixture of anatase and brookite, corresponding to a major phase of anatase (~95% estimated), with the smallest average crystallite size of 1.3 nm and the highest specific surface area (SSA) of 193 m^2/g. Furthermore, increasing TiO_2 concentration up to 0.4 molar for the sols prepared at 70°C resulted in decreasing the average crystallite size (1.9 nm at 300°C) and increasing SSA (116 m^2/g at 300°C) of the powders annealed at different temperatures. Anatase-to-rutile phase transformation temperature was increased with decreasing peptisation temperature down to 50°C, whereas TiO_2 concentration had no effect on this transition. Anatase percentage increased with decreasing both peptisation temperature and TiO_2 concentration. Such prepared powders can be used in many applications in areas from photo catalysts to gas sensors.

Keywords Anatase-TiO_2 · Sol-gel · Processing parameters · Characterisation

1. Introduction

Nanosized titania has a widespread range of applications, e.g. ultraviolet filters for optics and packing materials [1], antireflection coatings for photovoltaic cells and passive solar collectors [2], photo catalysts for purification and treatment of water and air [3], anodes for ion batteries [4], electrochromic displays [5], transparent conductors, self cleaning coatings on windows and tiles [6], humidity sensors [7] and gas sensors [8]. In developing gas sensors or catalyst systems it is critical to use a titania powder with the highest possible specific surface area. On the other hand, there is more supporting evidence in favour of anatase as the most promising for gas detection, as well as its catalyst application, due to its higher surface reactivity to gases [9, 10]. During the last years, many efforts have been aimed to produce nanosized titania powder with high specific

M. R. Mohammadi (✉) · M. C. Cordero-Cabrera · D. J. Fray
Department of Materials Science & Metallurgy,
University of Cambridge,
Pembroke Street, Cambridge CB2 3QZ, UK
e-mail: m_rz_mohammadi@yahoo.com or mrm41@cam.ac.uk

M. C. Cordero-Cabrera
e-mail: mcc40@cam.ac.uk

D. J. Fray
e-mail: djf25@cam.ac.uk

M. R. Mohammadi · M. Ghorbani
Department of Materials Science & Engineering and Institute for Nanoscience & Nanotechnology, Sharif University of Technology, Azadi Street, Tehran, Iran

M. Ghorbani
e-mail: ghorbani@sharif.ir

surface area using techniques such as sol-gel process, direct deposition from aqueous solutions [11], ultrasonic spray pyrolysis [12], laser-assisted pyrolysis [13], co precipitation method [14] and hydrothermal crystallisation [15].

For sol-gel, it is usually reported that high SSA is achieved by adding polymeric fugitive agents (PFAs). Examples are: Liu et al. [16] prepared crystallised anatase-TiO_2 powder, 4 nm grain size and 371.8 m^2/g BET area, by a modified sol-gel method with $Ti(NO_3)_4$ and polyethylene glycol with an average molecular weight of 2000 g/mol (PEG2000) and subsequent heat treatment at 100°C. Devi et al. [17] produced mixture of anatase and rutile crystallised TiO_2 powder with 9 nm average crystallite size and 88.9 m^2/g SSA heat treating at 500°C by using a modified sol-gel method with addition of PEG6000. Garzella et al. [18] reported mixture of anatase- and rutile-TiO_2 film annealed at 500°C with grain size less than 30 nm by chemically modified sol-gel procedure using hydroxypropyl cellulose. Keshmiri et al. [19] produced 75% anatase-TiO_2 powder annealed at 500°C with crystallite size of 19 nm and SSA of 34.3 m^2/g by composite sol-gel method using Degussa P-25 commercial titania powder as a filler mixed with the sol. Chen et al. [20] prepared mixture of anatase- and rutile-TiO_2 films annealed at 600°C with 40 nm grain size by sol-gel method using methylcellulose. Miki et al. [21] produced 10–20 nm TiO_2 powder annealed at 500°C by sol-gel method using trehalose dihydrate. Chemseddine et al. [22] produced antase-TiO_2 nanocrystals with 12 nm particle size using TTIP: Me_4NOH (tetramethylammonium hydroxide) = 1.14: 0.82 molar ratio by refluxing at 90–100°C for 6 h. Despite the fact that this technique has become one of the most widely used, not many studies report the production of high SSA by PFAs free sol-gel method. For example, Zhang et al. [23] reported 93% anatase-TiO_2 powder annealed at 500°C with the average particle size of 18 nm by a polymeric sol-gel method. Sivakumar et al. [24] prepared anatase-TiO_2 powder annealed at 600°C with 10.3 nm crystallite size and 104 m^2/g surface area from a titania sol. The titania sol was prepared by dispersing the precipitates, obtained from titanyl sulfate aqueous solution, into a mixture of hot distilled water and 10% HNO_3. Pottier et al. [25] produced nanoparticles of anatase-TiO_2 aged at 60° for a week with mean size in the range 5–10 nm by precipitation of $TiCl_4$ in aqueous medium in the range $2 \leq pH \leq 6$.

The effect of processing parameters on stabilisation of particulate titania sols was reported in a previous study [26]. Stable monomodal sols were obtained at peptisation temperature between 50°C and 70°C, for water/alkoxide molar ratios ranging from 250 to 1000 and acid/alkoxide molar ratios ranging from 0.4 to 0.7. It was found that peptisation temperature was the parameter with the greatest influence, followed by acid concentration, whereas the water/titania ratio showed little influence. This paper deals with the relation between stable sol preparation processing parameters (such as peptisation temperature and TiO_2 concentration) and the characteristics of powders obtained from these sols (such as phase structure, crystallite size, relative amount of phases, anatase-to-rutile phase transformation and the specific surface area). The influence of water/titania ratio, as well as peptisation temperature and acid/titania ratio, on characteristics of powders is reported in this study.

Table 1 Processing parameters and composition of TiO_2 sols

Sol (powder)	TiO_2 (molar)	HCl/TiO_2 (mol/mol)	H_2O/TiO_2 (mol/mol)	Peptisation temperature (°C)
TA-1	0.10	0.6	534	50
TA-2	0.20	0.5	258	70
TA-4	0.40	0.5	122	70

2. Experimental

2.1. Preparation of TiO_2 sols

Titanium tetraisopropoxide (TTIP) with a purity of 97% (Aldrich, UK) was used as precursor; analytical grade hydrochloric acid (HCl) 37% (Fisher, UK) was used as a catalyst for the peptisation and deionised water was used as a dispersing media. Three TiO_2 sols were prepared based on the optimised methodology reported before [26]. Table 1 shows details of the processing parameters and the molar ratio of sols.

For each sol, water-acid mixture (in the range of pH = 1–2) was stabilised at a constant temperature, and this temperature was kept throughout all the experiment, together with continuous stirring. TTIP was added next, forming a white thick precipitate, which gradually peptised after 2 h to form a clear sol. The clear sol was cooled to room temperature. Sols were characterised in particle size by dynamic light scattering technique (DLS) using a Malvern ZetaSizer 3000 HS at 20°C using a 10 mW He-Ne laser, 633 nm wavelength and 90° fixed scattering angle. The stability of prepared precursors was also determined by Zeta potential using the same instrument.

2.2. Synthesis of TiO_2 powders

Powders were prepared by drying each precursor at room temperature for 72 h under a fume cupboard with no special atmosphere. Afterwards all powders were heated at a rate of 5°C/min up to 300°C, 500°C and 800°C and held at these temperatures for 1 h in air. These powders were characterised in phase composition and crystallite size using an X-ray diffraction diffractometer (XRD) Philips E'pert PW3020,

Cu-K_α, and transmission electron microscope (TEM) JEOL 200CX. Since the brookite disappears at temperatures higher than 500°C, the mass fraction of rutile phase of powders annealed higher than that temperature can be calculated by the following equation [27]:

$$x_{\text{rutile}} = \frac{1}{1 + \text{K}(I_A/I_R)} \tag{1}$$

where I_A is the intensity of the anatase (101) reflection and I_R that of the rutile (110). The empirical constant K was determined via an XRD analysis of powders of known proportions of pure anatase and pure rutile, and is equal to 0.79. The anatase content of powders annealed at lower than 500 °C was estimated by the following equation:

$$Anatase = \frac{\sum_1^N I_{A_i}}{\sum_1^N I_{A_i} + \sum_1^N I_{B_j}} \tag{2}$$

where I_{A_i} is the intensity of the anatase reflections and I_{B_j} is the intensity of the brookite reflections. Based on TEM images of powders annealed at different temperatures, the spherical shape of particle was observed (see Section 3.4.2). It means the isotropic particles were obtained in this study. Thus, the crystallite size was calculated from the anatase (101), the brookite (121) and the rutile (110) reflections located at 25.4°, 30.8° and 27.4°, respectively, using the Debye-Scherrer equation [28]:

$$d = \frac{k\lambda}{B\cos\theta} \tag{3}$$

where d is the crystallite size, k a constant of 0.9, λ the X-ray wavelength of Cu which is 1.5406 A°, θ the Bragg's angle in degrees, and B the full width at half maximum (FWHM) of the peak. Powders were also characterised in microstructure using a scanning electron microscope FE-SEM JEOL 6340, thermal analysis using simultaneous differential thermal analysis TA-SDTQ600, with a heating rate of 5°C/min in air, chemical composition by Fourier transform infrared spectroscopy (FTIR) analysis using a Bruker Optics Tensor 27 analyser in the region 500–4000 cm^{-1}, and specific surface area by nitrogen absorption, from Brunauer-Emmett-Teller equation (BET) at 77.3 K using a Micromeritics Tristar 3000 analyzer. Prior to BET measurement, powders were degassed for 24 h at 40°C with pressure of 0.1 Pa. To prevent any possible crystallisation during outgassing, higher drying temperature was avoided. The average grain size of the films was determined by both FE-SEM micrographs and following equation [16]:

$$D = \frac{6000}{s\rho} \tag{4}$$

where D (nm) is the average grain size, s (m^2/g) is the specific surface area and ρ (g/cm^3) is the density of anatase or rutile (3.85 and 4.25 g/cm^3, respectively).

3. Results and discussion

3.1. Particle size

Figure 1 shows the average hydrodynamic size of the TiO_2 particles in prepared sols, being 13 nm, 28 nm and 20 nm for TA-1, TA-2 and TA-4 sols, respectively. The hydrodynamic diameter of TiO_2 particles in sols is affected by ionic strength of medium because various HCl concentrations were used. The higher HCl/TiO_2 molar ratio, the higher the surface charge around the particles, resulting in preventing coagulation and flocculation of particles by electrostatic repulsion. Consequently, TA-1 sol had the smallest particle size among all sols. There is a limit to this behaviour, as an excess of HCl can compress the double layer to such extent that interparticle distance is reduced during collisions, resulting in agglomeration [26]. Therefore, optimum HCl concentration is required in order to break down the particles into small ones during peptisation. Nevertheless, all of the three sols had nanosize TiO_2 particles. Moreover, TA-4 sol showed less particle size than TA-2 sol. Consequently, both HCl and TiO_2 concentration have important effect on particle size. Compared to the titania sol prepared by Sivakumar et al. [24] (with TiO_2 average particle size of 30 nm), TA-1 and TA-4 sols showed smaller TiO_2 particle size arising from a much more straightforward preparation method.

3.2. Zeta potential

The average zeta potential of sols is shown in Fig. 2. The stability of these sols was achieved by electrostatic repulsion or surface charge stabilisation mechanism. This mechanism has effect on particles interaction due to the distribution of charged species in the sol. It has been reported that generally speaking the range of zeta potential in unstable sols goes from –30 to +30 mV [29]. The zeta

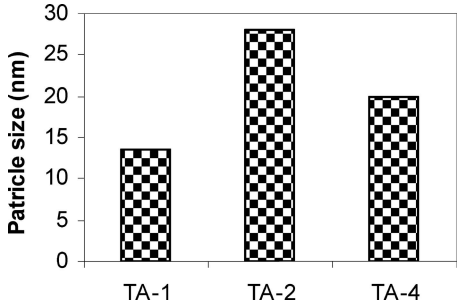

Fig. 1 The mean hydrodynamic size of the TiO_2 particles in sols

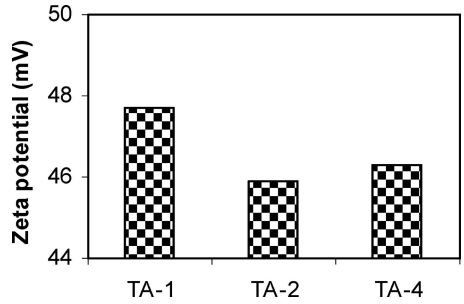

Fig. 2 Zeta potential of TiO_2 particles in prepared sols (pH = 1–2)

potential of TiO_2 particles in TA-1, TA-2 and TA-4 sols was 47.7 mV, 45.9 mV and 46.3 mV, respectively. Therefore, there is no drastic difference between them. As mentioned before, the surface charge around the particles of TA-1 sol is higher than that of for the other sols, thus resulting in higher zeta potential. All sols were found to be stable over 7 months. Pottier et al. [25] studied the influence of pH on the surface charge density of TiO_2 particles synthesised by precipitation from $TiCl_4$ in aqueous medium. It decreased with increasing pH from 2 to 6 in due to the same reason described in the previous section.

3.3. Infrared characteristic

Figure 3 shows the IR spectra of as-synthesized TA-4 powder dried at room temperature for 72 h. The characteristic absorption peak of (OR) group of titanium isopropoxide, which was the precursor of the sols, is in range 1085–1050 cm^{-1} [30]. Owing to the fact that no absorption peak was detected in this range, it shows that all of the four (OR) groups of titanium isopropoxide were substituted with (OH) groups of water. As expected, a full conversion of TTIP is obtained by the hydrolysis reaction, resulted in formation of TiO_2 particles. The water incorporation is found with the group peaks between 1643–1627 cm^{-1}, characteristic of stretching vibration H-O-H band [31]. Moreover, the broad band centered at

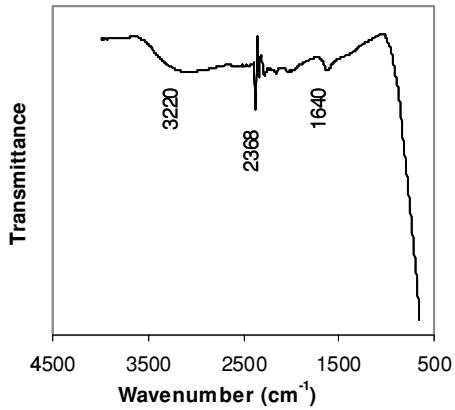

Fig. 3 FT-IR spectrum of as-synthesized TA-4 powder

3220 cm^{-1} is due to the stretching vibration of the hydroxyl (O-H) bond. The absorption peak at 2368 cm^{-1} is assigned to the influence of the CO_2 of the environment during measurement. Similar results were obtained for TA-2 and TA-4 as-synthesized powders.

3.4. Crystal characterisation

3.4.1. XRD analysis

The X-ray diffraction pattern of as-synthesized and annealed at 300, 500 and 800°C of TA-1 powders is shown in Fig. 4. It is clear that crystallisation of anatase and brookite has already occurred at room temperature, resulting in very fine crystallite size. Anatase disappears at temperatures higher than 800°C, whereas brookite disappears at temperatures higher than 500°C. Moreover, broad diffraction peaks imply small crystallite size of as-synthesized and annealed below 300°C powders. Formation of rutile phase was observed in powders annealed at 500°C and higher. The strongest peak observed for anatase, brookite and rutile phases at different temperatures were (101) $2\theta = 25.4°$, (121) $2\theta = 30.8°$ and (110) $2\theta = 27.4°$, respectively. Therefore, formation of rutile phase together with the anatase phase at low temperature was found as a result of the peptisation achieved by the HCl. This can be ascribed by the presence of hydroxyls within the as-synthesised powders (as confirmed by IR spectra in Section 3.3). When powders were annealed, the dehydroxylation generated lattice defects that produced microstrains and

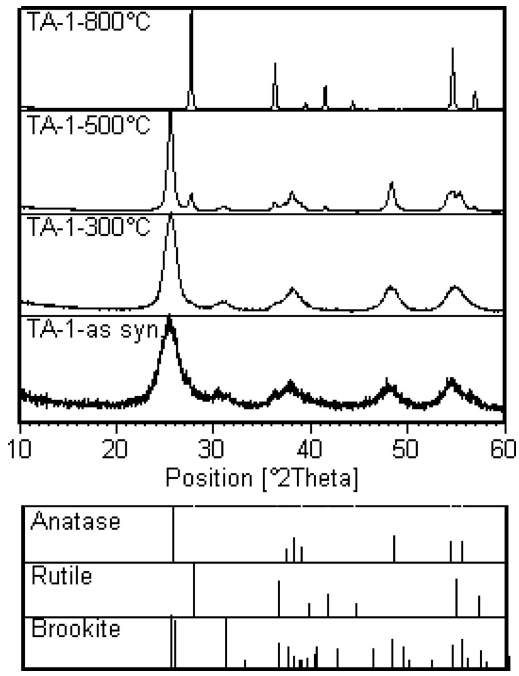

Fig. 4 XRD patterns of TA-1 powder: as-synthesized and annealed at 300, 500 and 800°C for 1 h

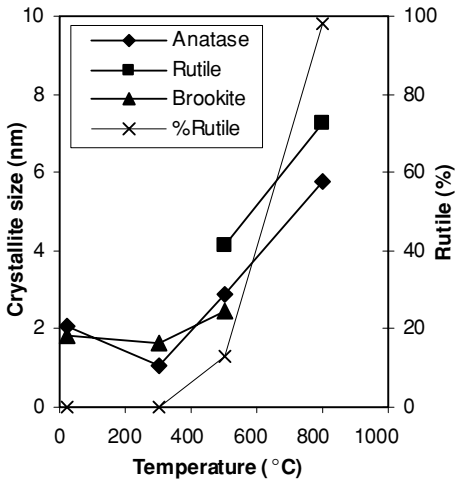

Fig. 5 Crystallite size of anatase, rutile and brookite and percentage of rutile phase of TA-1 powders annealed at different temperatures for 1 h

created conditions for rearrangement of parallel octahedral in the case of anatase (octahedrals that are connected by their vertices) to 90° rotated octahedral in the case of rutile (octahedrals that are connected by their edges). Therefore, phase transformation from anatase-to-rutile can be regarded in terms of reconstructive polymorphism with symmetry change from $I4_1/amd$ to $P4_2/mnm$ space group [32, 33]. This phenomenon has been previously observed by Bokhimi et al. [34] using titanium trichloride in an acid- and oxygen- rich environment. Figure 5 shows the effect of annealing temperature on rutile content and crystallite size of TA-1 powders.

It is important to remember, DLS is measuring particles, which in this case are conformed of aggregated of various crystallites. Based on Eq. (2), 300°C annealed TA-1 powder showed 95% anatase-TiO_2 phase with the average crystallite size of 1.3 nm. The anatase and brookite crystallite sizes of as-synthesized powder, (2.1 nm and 1.8 nm, respectively) decreased after annealing at 300°C, (1.0 nm and 1.6 nm, respectively). The reason of this phenomenon can be explained by removal of crystallisation water of as-synthesized powder, whose presence has been confirmed by FTIR. This result was also confirmed by SDT analysis, as shown in Section 3.5. Although, the average crystallite size of powder increased gradually with increasing annealing temperature to higher than 300°C, the average crystallite size of 800°C annealed powder was 6.5 nm, which shows good thermal stability. Zhang et al. [23] reported mixture of 35 nm anatase size and >100 nm rutile size for powder annealed at 550°C by a sol-gel method with peptisation temperature of 50°C. Sivakumar et al. [24] prepared mixture of 22 nm anatase size and 27.2 nm rutile size (92.8% rutile phase) for powder annealed at 800°C. Devi et al. [17] reported 3.8 nm crystallite size for mesoporous of as-synthesized TiO_2 powder prepared by a modified sol-gel with $Ti(NO_3)_4$ and PEG6000. Keshmiri et al. [19] produced TiO_2-based powders annealed at 500°C with crystallite size of 16 nm by a composite sol-gel method. Chen et al. [20] reported 40 nm TiO_2 particles annealed at 600°C by a sol-gel method by using methylcellulose. Liu et al. [16] prepared 4 nm anatase-TiO_2 powder by a modified sol-gel method using $Ti(NO_3)_4$ and PEG2000 and subsequent heat treatment at 100°C.

Consequently, we succeed to produce the TiO_2 powders with higher anatase content and lower crystallite size than those reported in previous studies which used sol-gel method, even though no PFAs were used. Moreover, crystallite size of powders reported in this study is also lower than that of reported by previous authors using other methods: Ruiz et al. [15] synthesized 20 nm TiO_2 powder with mixture of anatase and rutile phases annealed at 700°C by hydrothermal treatment. The smallest TiO_2 crystallite size produced by Pottier et al. [25], under conditions of pH = 2 and aging of the precipitation of $TiCl_4$ in aqueous medium at 60°C for a week, was 5.5 nm. Crystallite size of TiO_2 nanocrystal prepared by Chemseddine et al. [22] using Ti: Me_4NOH = 1.14: 0.82 molar ratio and refluxed at 200°C for 6 h was 12 nm. They also studied the effect of autoclave temperature on TiO_2 crystallite size. It was observed that decreasing the autoclave temperature from 200 to 175°C resulted in increasing TiO_2 crystallite size from 12 to 18 nm.

Figure 6 shows X-ray diffraction pattern of TA-1, TA-2 and TA-4 powders annealed at 300°C (Fig. 6(a)) and 500°C (Fig. 6(b)) for 1 h. Moreover, the average crystallite size and rutile percentage of these powders is shown in Fig. 7. It can be concluded that the rutile percentage increased with increasing peptisation temperature during sol preparation, especially for powders annealed at high temperatures. Consequently, for applications such as photo catalyst and gas sensing, where anatase is the preferred phase, decreasing peptisation temperature for sol preparation is necessary.

A comparison between the results of particle size of sols and the average crystallite size for powders leads to the conclusion that, the lower the particle size in sol, the smaller the crystallite size after heat treatment of the powder. Thus, the variation in crystallite size is closely related to the variation in the electrostatic surface charge density of the nanoparticles. This phenomenon has been previously observed by Pottier et al. [25]. Moreover, based on results of average crystallite size and rutile percentage it can be concluded that an increase in the rutile content does not necessarily induce an increase on the average crystallite size, since a new phase is being formed. Therefore, TiO_2 concentration proved to be more influential on crystallite size than the anatase/rutile ratio.

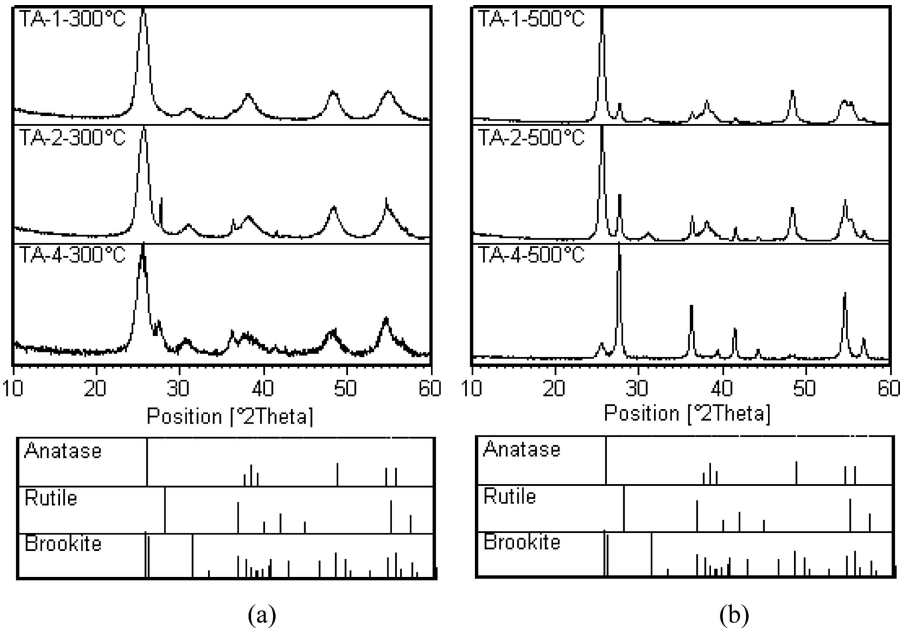

Fig. 6 XRD patterns of TA-1, TA-2 and TA-4 powders annealed at (a) 300°C and (b) 500°C for 1 h

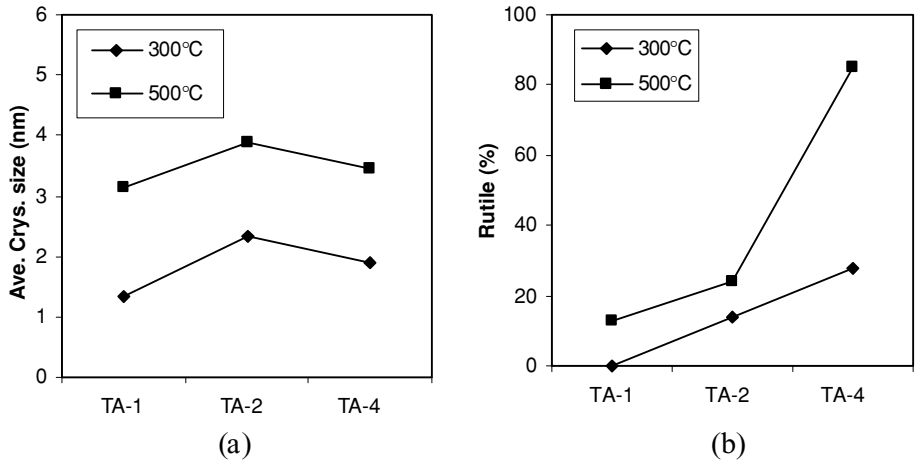

Fig. 7 (a) Average crystallite size and (b) rutile percentage of TA-1, TA-2 and TA-4 powders annealed at 300°C and 500°C for 1 h

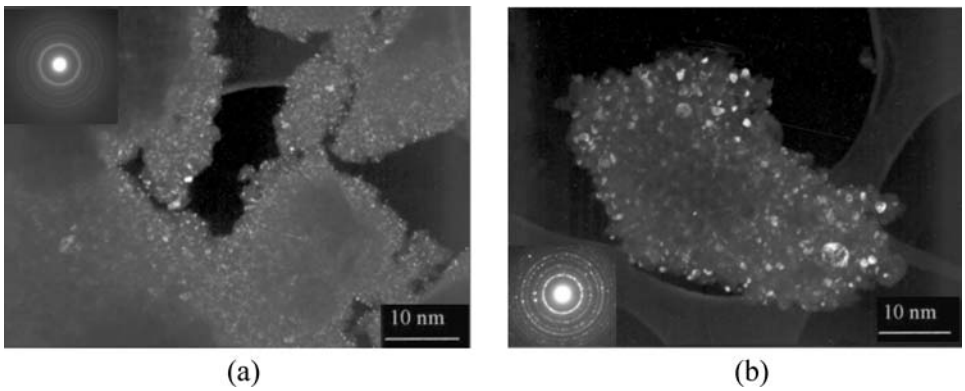

Fig. 8 TEM analysis: (a) dark-field plane-view image of as-synthesized TA-1 powder. The inset shows the typical well defined rings arising from crystallite structures. (b) dark-field plane-view image of 500°C annealed TA-1 powder. The inset shows the typical well defined rings arising from crystallite structures

3.4.2. TEM analysis

Figure 8 highlights the selected area diffraction pattern (SADP) of as-synthesized and 500°C annealed TA-1 powder. As seen in Fig. 8(a), as-synthesized TA-1 powder exhibited high uniformity in particle size. Furthermore, the inset shows the typical well defined rings arising from crystallite structures with crystallite size of around 1 nm, which is in good agreement with those obtained by XRD analysis. The measured interplanar distances agree with the expected values

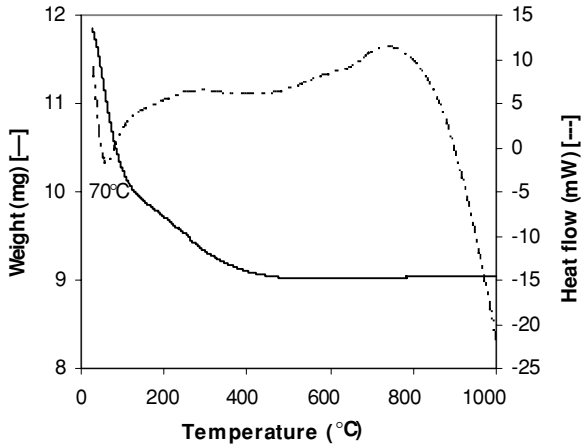

Fig. 9 SDT curve of TA-1 powder dried at 25°C for 72 h. The scan rate was 5°C/min, performed in air

reported for anatase-TiO_2 [35]. Figure 8(b) revealed that annealing at 500°C induced a gradual increase in crystallite size up to 3 nm.

3.5. Thermal analysis

Simultaneous differential thermal analysis (SDT) of TA-1 powder is shown in Fig. 9. It is seen that prepared powder undergoes endothermic dehydration in the temperature range 25–70°C. An exothermic broad peak in range 70–450°C shows the crystallisation of anatase- and brookite-TiO_2 structures and the next exothermic vast broad peak in the temperature range 500–850°C shows the crystallisation of rutile-TiO_2 structure.

The TGA curve shows that the weight loss occurs at two stages, namely, below 130°C and between 200 and 500°C. In the first region (below 130°C), the weight loss of 14.3% is believed to be a result of the evaporation of water. In the second stage, the weight loss of 9.4% is probably ascribed to the evaporation of water of crystallisation or transformation from titanium hydroxide to oxide. Note that the presence of OH groups (either from H_2O or $Ti(OH)_4$) has been confirmed by IR spectra (see Section 3.3.). Similar curves were obtained for TA-2 and TA-4 as-synthesized powders.

3.6. Microstructure

Figure 10 shows FE-SEM micrographs of TA-1, TA-2 and TA-4 powders annealed at 500°C. It can be observed that in all cases nanometer TiO_2 powders were obtained. The average grain size of the powders, determined by FE-SEM image analysis, as a function of temperature is shown in Fig. 11. These results are in good agreement with the values calculated with Eq. (3). The average grain size of powders annealed at 500°C is around 10 nm, 19 nm and 15 nm for TA-1, TA-2 and TA-4 powders, respectively.

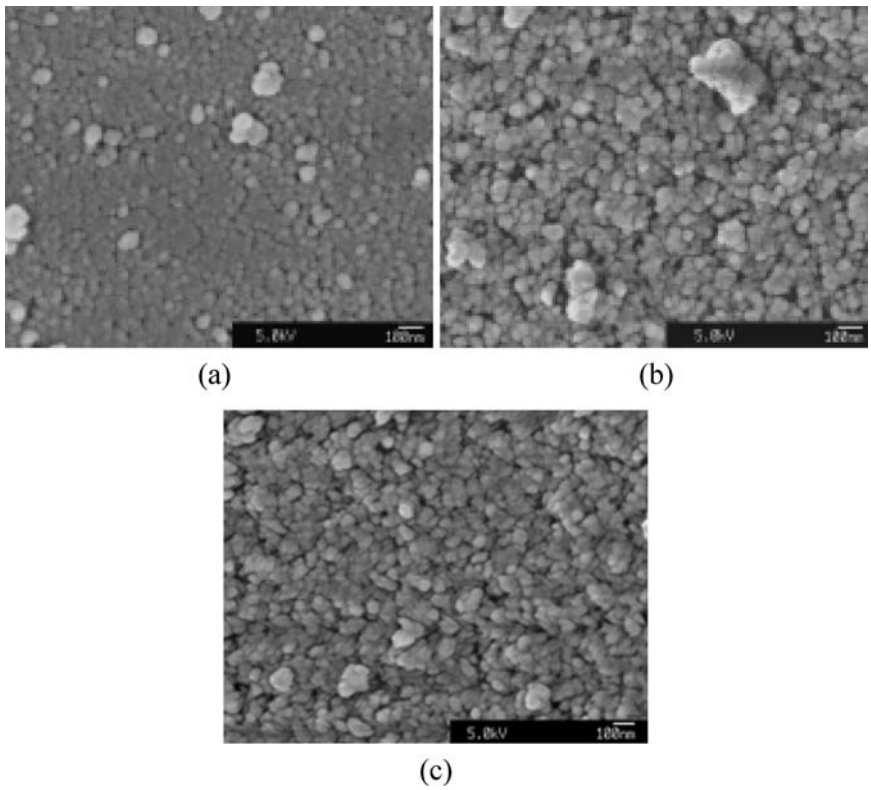

Fig. 10 FE-SEM images of the surface morphology of 500°C annealed powders: (a) TA-1, (b) TA-2 and (c) TA-4

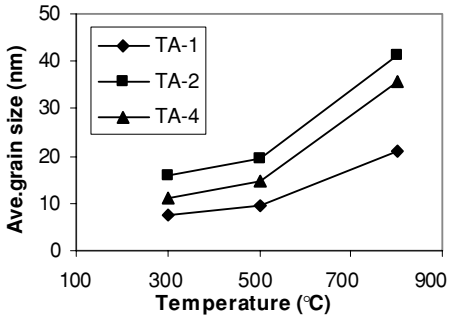

Fig. 11 Average grain size of TA-1, TA-2 and TA-4 powders as a function of annealing temperature

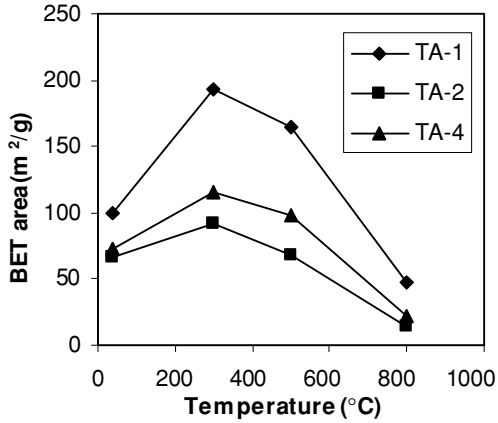

Fig. 12 BET surface area of TA-1, TA-2 and TA-4 powders annealed at different temperatures for 1 h

3.7. Specific surface area of powders

Figure 12 shows the specific surface area of as-synthesized and annealed powders at 300°C, 500°C and 800°C for 1 h. The SSA of as-synthesized powders were in the range 66–99 m^2/g and once the powders are subjected to heat treatment, increasing the annealing temperature up to 300°C for 1 h, an increase of the BET area was seen: 193 m^2/g, 91 m^2/g and 116 m^2/g for TA-1, TA-2 and TA-4, respectively. Again, this phenomenon is related to the water evaporation when the powders are heat treated (as shown in Section 3.5.). A decrease in SSA was observed with increasing annealing temperature up to 800°C due to grain growth (47 m^2/g for TA-1, 14 m^2/g for TA-2 and 21 m^2/g for TA-4). This result is in good agreement with the average crystallite size and particle size of the sol. Thermal stability of the prepared powders is higher than that of prepared by Sivakumar et al. [24] who obtained the BET area of 374.8 m^2/g for 200°C annealed TiO_2 powder. The BET area of this powder decreased down to 9.1 m^2/g after annealing at 800°C. Although high surface area TiO_2-based powders have been reported by other authors, different additives were used in their studies such as polyethylene glycol, chitason, methylcellulose and etc. The BET area of as-synthesized TiO_2 powder has been produced by Liu et al. [16] using $Ti(NO_3)_4$ and PEG2000 was 317.8 m^2/g. Devi et al. [17] produced TiO_2 powder annealed at 500°C using $Ti(NO_3)_4$ and PEG6000 with BET area of 88.9 m^2/g. Miki et al. [21] reported 163 m^2/g BET area of TiO_2 powder annealed at 500°C and prepared by sol-gel method using 0.015 kg trehalose dihydrate/L. Keshmiri et al. [19] prepared 75% anatase-TiO_2 powder annealed at 500°C with crystallite size of 19 nm and SSA of 34.3 m^2/g by composite sol-gel method using Degussa P-25 commercial titania powder as a filler mixed with the sol. To the best of our knowledge, there is no report about production of high SSA TiO_2 powders by additive free sol-gel technique. Consequently, we succeeded in preparing one of the highest SSA additive free TiO_2 powders by controlling sol preparation processing parameters. Owing to the fact that, these sols showed good ability of dissolving polymeric fugitive agents (PFAs) (such as trehalose dihydrate, polyethylene glycol and hydroxypropyl cellulose) in order to produce high surface area titania powders, we studied the effect of those PFAs on characteristics of nanoporous and nanosized TiO_2-based films and powders and reported results elsewhere [36–38].

4. Conclusions

Nanocrystalline titanium dioxide powders were obtained from stable sols produced using particulate sol-gel route in various processing parameters. The sol prepared at 50°C and 0.1 M showed the smallest hydrodynamic size of TiO_2 particles (13 nm) and the highest stability among all the sols. In addition, the powders obtained from this sol had the smallest crystallite size (1.3 nm), the highest anatase percentage (~95%) and the highest SSA (193 m^2/g) at 300°C. It was found that the average crystallite size and the average grain size of powders were decreased with decreasing peptisation temperature down to 50°C during preparation of sol, thus resulting in increasing the SSA of powders. Moreover, anatase-to-rutile phase transformation temperature was increased with decreasing peptisation temperature down to 50°C, while TiO_2 concentration had no effect on this transition. TiO_2 concentration was proved to be much more important than the anatase/rutile ratio on the average crystallite size. Since the anatase-TiO_2 with high SSA and small grain size is a favour phase for gas sensors and photo catalysts, such powders prepared in this work are recommended for those applications.

Acknowledgments The authors wish to acknowledge Mr. David Nicol for his help with TEM analysis. M.R. Mohammadi and M. Ghorbani would like to acknowledge British Council in Iran, Iranian's Ministry of Science, Research and Technology and Center of Excellence for Nano Structures (CENS) for their financial support.

References

1. Bonini N, Carotta MC, Chiorini A, Guidi V, Malagu C, Martinelli G, Paglialonga L, Sacerdoti M (2000) Sensors Actuators B 68:274
2. Perera VPS, Jayaweera PVV, Pitigala PKDDP, Andaranayake PKMB, Hastings G, Perera AGU, Tennakone K (2004) Synth Met 143:283
3. Mao D, Lu G, Chen Q (2004) Applied Catalysis A: General 263:83
4. Huang Y, Kavan L, Exnar I, Gratzel M (1995) J Electrochem. Society 142:L142
5. Aliev AE, Shin HW (2002) Displays 23:239
6. Fretwell R, Douglas P, (2001) Photochem J Photobiol A: Chem 143:229
7. Tai WP, Oh JH (2002) Sensors and Actuators B 85:154
8. Francioso L, Presicce DS, Taurino AM, Rella R, Siciliano P, Ficarella A (2003) Sensors Actuators B 95:66
9. Inagaki M, Nakazawa Y, Hirano M, Kobayashi Y, Toyoda M (2001) J Inorg Mater 3:809
10. Tanner RE, Liang Y, Altman EI (2002) Surface Science 506:251
11. Shimizu K, Imai H, Hirashima H, Tsukuma K (1999) Thin Solid Films 351:220
12. Blesic MD, Saponjic ZV, Nedeljkovic JM, Uskokovic DP (2002) Mater Lett 54:298
13. Carotta MC, Ferroni M, Gnani D, Guidi V, Merli M, Martinelli G, Casale MC, Notaro M (1999) Sensors Actuators B 58:310
14. Lee DS, Han SD, Huh JS, Lee DD (1999) Sensors Actuators B 60:57
15. Ruiz AM, Arbiol J, Cornet A, Shimanoe K, Morante JR, Yamazoe N (2005) Mater Res Soc 828:A4.10.1
16. Liu X, Yang J, Wang L, Yang X, Lu L, Wang X (2000) Mater Sci Engi A 289:241
17. Devi GS, Hyodo T, Shimizu Y, Egashira M (2002) Sensors Actuators B 87:122
18. Garzella C, Comini E, Tempesti E, Frigeri C, Sberveglieri G (2000) Sensors Actuators B 68:189
19. Keshmiri M, Mohseni M, Troczynski T (2004) Applied Catalysis B: Environmental 53:209
20. Chen W, Zhang J, Fang Q, Li S, Wu J, Li F, Jiang K (2004) Sensors Actuators B 100:195
21. Miki T, Nishizawa K, Suzuki K, Kato K (2004) Mater Lett 58:2751
22. Chemseddine A, Moritz T (1999) Eur J Inorg Chem 235
23. Zhang H, Finnegan M, Banfield JF (2001) Nano Letters 1:81
24. Sivakumar S, Krishna Pillai P, Mukundan P, Warrier KGK (2002) Mater Lett 57:330
25. Pottier A, Cassaignon S, Chaneac C, Villain F, Tronc E, Jolivet JP (2003) J Mater Chem 13:877
26. Cordero-Cabrera MC, Walker GS, Grant D (2005) J Mater Sci 40:3709
27. Spurr R, Myers H (1957) Anal Chem 29:760
28. Cullity BD (1978) Elements of X-ray diffraction, Addison-Wesley Publishing Company Inc, London, p 99
29. Malvern instruments (2003) DST customer training manual for zeta potential, chapter 6
30. Socrates G (1994) Infrared characteristic group frequencies: Tables and charts, Second Edition John Wiley & Sons, England, p 62/237
31. Ivanova T, Harizanova A, Surtchev M (2002) Mater Lett 55:327
32. Carp O, Huisman CL, Reller A (2004) Progress in Solid State Chemistry 32:33
33. Diebold U (2003) Surface Science Reports 48:53
34. Bokhimi X, Morales A, Pedraza F (2002) J Solid State Chem 169:176
35. JCPDS PDF-2pattern 73–1764
36. Mohammadi MR, Cordero-Cabrera MC, Fray DJ, Ghorbani M, (2006) In Press in Journal of Sensors Actuators B
37. Mohammadi MR, Ghorbani M, Fray DJ (2006) In Press in J Mater Sci Techn
38. Mohammadi MR, Ghorbani M, Cordero-Cabrera MC, Fray DJ (2006) In Press in J Mater Sci